

Adiabatic Heuristic Principle on a Torus and Generalized Streda Formula

Koji Kudo¹ and Yasuhiro Hatsugai^{1,2}

¹Graduate School of Pure and Applied Sciences, University of Tsukuba, Tsukuba, Ibaraki 305-8571, Japan

²Department of Physics, University of Tsukuba, Tsukuba, Ibaraki 305-8571, Japan

(Dated: September 11, 2020)

Although the adiabatic heuristic argument of the fractional quantum Hall states has been successful, continuous modification of the flux/statistics of anyons is strictly prohibited due to algebraic constraints of the braid group on a torus. We have numerically shown that the adiabatic heuristic principle for anyons is still valid even though the Hamiltonians cannot be modified continuously. The Chern number of the ground state multiplet is the adiabatic invariant, while the number of the topological degeneracy behaves wildly. A generalized Streda formula is proposed that explains the degeneracy pattern. Nambu-Goldstone modes associated with the anyon superconductivity are also suggested numerically.

I. INTRODUCTION

Over the past decade, topology has been coming to the fore in modern condensed matter physics. The quantum Hall (QH) effect^{1,2} is a prime example of topologically non-trivial phases, where the quantized Hall conductance is given by the Chern number³⁻⁶. Topological concepts enrich material phases beyond the Ginzburg-Landau theory. The fractional QH (FQH) state⁷ is a typical example of the quantum liquid with the topological order⁸. It hosts fractionalized excitations that carry fractional charges and fractional statistics⁹⁻¹¹, which is the hallmark of the topologically ordered phases¹². The topological degeneracy is closely related to these fractionalizations^{8,13-15}. Some of the non-Abelian topological order can be used for a possible quantum computation¹⁶⁻²⁰.

Point particles in two-dimension can be charge-flux composites associated with a singular gauge transformation²¹. In relation to the composite fermion picture^{22,23}, the flux-attachment has been quite successful to describe the FQH effect; the FQH effect at the filling factor $\nu = p/(2mp \pm 1)$ with p and m integers can be understood as the $\nu = p$ IQH effect of the composite fermions. This concept is further developed to the “adiabatic heuristic principle”^{24,25}. It states that both states are adiabatically connected through intermediate systems of anyons. This characterization of the QH states based on the adiabatic deformation is a typical example of the topological classification as is widely applied to the recent studies of topological phases.

We note that a careful setup is required to carry the program of this adiabatic heuristic principle for concrete systems. The statistical phase θ of anyons is governed by a representation of the fundamental group of the many-particle configuration space (braid group)²⁶. Therefore, the world lines of the system needs to satisfy the braid group constraint.

As for topological phenomena, the geometry of the system is crucially important. With boundaries, low energy modes appear as edge states even for gapped systems. Thus, for the demonstration of the adiabatic heuristic principle, the torus geometry without any boundaries is favorable²⁷. However, an algebraic constraint of

the braid group on a torus^{13,28-32} prohibits continuous change of the statistical phase θ . This makes it impossible to apply the adiabatic heuristic principle naively.

In this Letter, we show that the adiabatic heuristic principle indeed remains valid on a torus. Here, “adiabatic” is used in the sense that the gap remains open although continuous deformation of the Hamiltonian is impossible. The many-body Chern number of the ground state multiplet is also calculated numerically, which serves as the adiabatic invariant while their degeneracy changes wildly. We propose a generalized Streda formula to characterize the obtained degeneracy pattern in relation to the Chern number, which follows from the translational invariance of anyons. At the gap closing point, the Chern number changes its sign and the anyon superconductivity³³⁻³⁵ is expected.

II. ADIABATIC HEURISTIC PRINCIPLE AND BRAID GROUP

Let us here shortly derive the fundamental relation of the adiabatic heuristic principle^{24,25}. We consider a QH system of N_a particles with the charge $-e$ in a uniform magnetic field. According to the adiabatic heuristic principle, the QH state is adiabatically deformed by trading the external fluxes for the statistical ones of anyons. Since the total flux remains constant ($N_\phi + N_a\theta/\pi = \text{const.}$), one has the relation $1/\nu + \theta/\pi = \text{const.}$, where N_ϕ is the number of the external flux, θ is the statistics of anyons and $\nu = N_a/N_\phi$. Assuming that the $\nu = p$ IQH state of fermions ($\theta = \pi$) is included in this series, one has $\nu = p/[p(1 - \theta/\pi) + 1]$.

From the analysis of the braid group on a torus^{13,28-32}, the relation $1/\nu + \theta/\pi = \text{const.}$ is rederived (see Appendix A) with an *additional* constraint as explained below. The generators of the braid group on a torus are denoted as σ_i , τ_i and ρ_i , where σ_i ($i = 1, \dots, N_a - 1$) is a local exchange between the i th and $i + 1$ th anyons, and τ_i and ρ_i ($i = 1, \dots, N_a$) are global moves of the i th anyon along a noncontractible loop on the torus in x and y directions. Now, we take the basis $|\{\mathbf{r}_k\}; w\rangle$ for their expressions, where $\{\mathbf{r}_k\}$ is the positions of anyons and

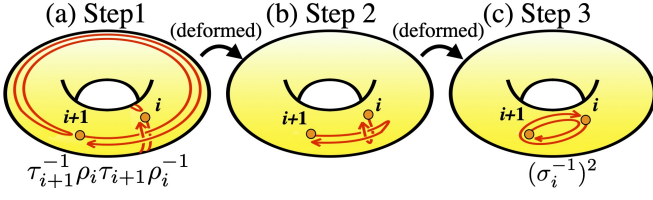


FIG. 1. Pictorial proof of Eq. (1)²⁸. (a) The paths of the four moving processes ρ_i^{-1} , τ_{i+1} , ρ_i , and τ_{i+1}^{-1} are presented in the order from bottom to top. (c) The path in (a) can be deformed into that of $(\sigma_i^{-1})^2$.

$w = 1, \dots, M$ is the extra internal index that is necessary to satisfy the braid group constraints on a torus as seen below. We assume that anyons are Abelian: $\sigma_i = e^{i\theta} \mathbf{1}_M$, where $\mathbf{1}_M$ is the M -dimensional unit matrix. As shown in Fig. 1²⁸, the generators σ_i , τ_i and ρ_i need to satisfy

$$\tau_{i+1}^{-1} \rho_i \tau_{i+1} \rho_i^{-1} = (\sigma_i^{-1})^2 = e^{-i2\theta} \mathbf{1}_M. \quad (1)$$

By taking a determinant of Eq. (1), we have $1 = e^{-i2M\theta}$. If $\theta/\pi = n/m$ (with n, m coprime), the dimension of the representation M needs to be a multiple of m . This constraint strictly prohibits continuous change of the Hamiltonian in the adiabatic heuristic principle.

In this Letter, this puzzle is resolved. Although the Hamiltonian is defined only for discrete values of θ and its dimension behaves wildly, the energy gap defined by a dense set of the Hamiltonians is surprisingly smooth and finite. It justifies the adiabatic heuristic principle on a torus. We also find the generalized streda formula to explain the wild behavior of the degeneracy by the many-body Chern number.

III. MODEL

We consider the periodic system of anyons in the uniform magnetic field on a square lattice with $N_x \times N_y$ sites. The Hamiltonian is

$$H = t \sum_{\langle ij \rangle} e^{i\phi_{ij}} e^{i\theta_{ij}} c_i^\dagger c_j \otimes W^{(ij)} + V \sum_{\langle ij \rangle} n_i n_j \otimes \mathbf{1}_M, \quad (2)$$

where $n_i = c_i^\dagger c_i$ and c_i^\dagger (c_i) is the creation (annihilation) operator for a hard-core boson on site i . The hard-core condition is necessary to ensure consistency with the braid group. The Peierls phase $e^{i\phi_{ij}}$ is specified by the string gauge³⁶ for the external magnetic field. The phase $e^{i\theta_{ij}}$ describes the statistical phase^{29,30} (see the details below). $W^{(ij)}$ is an M -dimensional matrix³⁰ to ensure consistency with Eq. (1). When $\theta/\pi = n/m$, M is fixed to be m as the irreducible representation. We set $W^{(ij)} = W_x$ and W_y for (ij) describing a pair of sites across the boundary in the x and y directions respectively

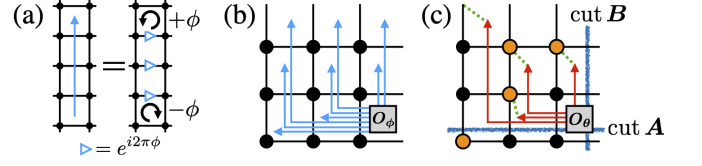


FIG. 2. (a) String gauge. (b)(c) Sketches of 3×3 square lattice with (b) the string gauge ϕ_{ij} and (c) the statistical gauge θ_{ij} . The yellow points in (c) represent sites with anyons.

and otherwise $W^{(ij)} = \mathbf{1}_M$, where

$$W_x = \begin{bmatrix} 0 & 1 & \dots & 0 \\ \vdots & \vdots & \ddots & \vdots \\ 0 & 0 & \dots & 1 \\ e^{i\eta_x} & 0 & \dots & 0 \end{bmatrix}, \quad (3)$$

$$W_y = e^{i\eta_y} \text{diag}[e^{i2\theta}, e^{i4\theta}, \dots, e^{i2M\theta}], \quad (4)$$

and $\vec{\eta} = (\eta_x, \eta_y)$ specifies the twisted boundary conditions. The Hamiltonian is consistent with Eq. (1) since we have $W_x^{-1} W_y W_x W_y^{-1} = e^{-i2\theta} \mathbf{1}_M$ for any $\vec{\eta}$.

Let us now give detailed descriptions of how to construct the Hamiltonian in Eq. (2). We first mention the string gauge ϕ_{ij} briefly. As shown in Fig. 2(a), let us consider a string on sites and assigns the Peierls phase $e^{i2\pi\phi}$ on the links intersected by the string. They clearly describe the magnetic fluxes ϕ and $-\phi$ at the initial and terminal points of the string, respectively. Thus, the string gauge shown in Fig. 2(b) introduces the flux $\phi \times (1 - N_x N_y)$ to the plaquette with the origin O_ϕ while ϕ to the others. The gauge convention θ_{ij} is also described by the strings, see Fig. 2(c). The strings carry the phase factor $e^{i\theta}$, and their terminal points are located at plaquettes adjoining anyons. Besides, the additional rules are given as follows³⁰: (The roles of each rule are explained in Ref. 37)

(i) If a string sweeps another anyon in the process of hopping, one determines the phase factor as if the anyon crosses the string.

(ii) When an anyon hops across the cut B from left to right, the phase factor $e^{i(N_a - 1)\theta}$ is given.

(iii) When an anyon hops across a horizontal string, the phase factor not $e^{i\theta}$ but $e^{i2\theta}$ is given.

(iv) When an anyon hops across the cut A upward, the phase factor $e^{iX\theta}$ is given, where X is the number of other anyons in the same x -axis position as the hopping anyon.

Due to Eqs. (3) and (4), we also give the following rules: When an anyon hops across the cut B from left to right, the label is changed from w to $w - 1$, where w is the label of the basis $|\{\mathbf{r}_k\}; w\rangle$. If $w = 1$, the phase factor $e^{i\eta_x}$ is also given. Also, when an anyon hops across the cut A upward, the phase factor $e^{i\eta_y} e^{i2w\theta}$ is given.

In this framework, the representations of the global move operators are given as $\tau_j = e^{i\frac{\epsilon}{\hbar} \alpha_j} e^{-i2\theta(j-1)} W_x$ and $\rho_j = e^{i\frac{\epsilon}{\hbar} \beta_j} e^{i2\theta(j-1)} W_y$, where $e^{i\frac{\epsilon}{\hbar} \alpha_j}$ and $e^{i\frac{\epsilon}{\hbar} \beta_j}$ are came

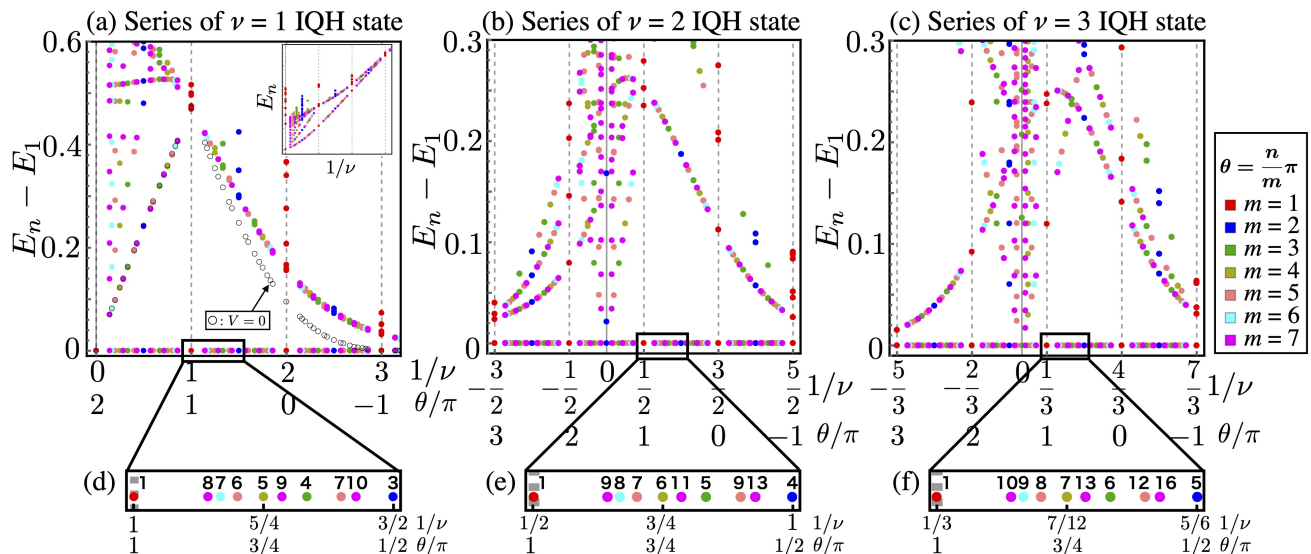


FIG. 3. (a-c) Energy gaps are shown as functions of $1/\nu$ for $t = -1$ and $V = 5$. The system size is $N_x \times N_y = 10 \times 10$. The statistical parameter θ is determined by $\nu = p/[p(1 - \theta/\pi) + 1]$ with (a) $p = 1$ (b) $p = 2$, and (c) $p = 3$, respectively. The vertical dashed lines represent $\theta/\pi = \text{integer}$. The anyon number is (a),(b) $N_a = 4$ and (c) $N_a = 3$. We plot the lowest N_{cut} states at each $1/\nu$ in the figures [$N_{\text{cut}} = 40$ for (a) and (b), and $N_{\text{cut}} = 70$ for (c)]. The open black circles in (a) are the gaps $E_{N_D+1} - E_1$ for $V = 0$. The inset in (a) is the energy spectrum of the same setting as (a). (d-f) Ground state degeneracy N_D is shown.

from the Peierls phase ϕ_{ij} describing the external magnetic field. As shown in Appendix A, these representations are consistent with the braid group on a torus.

The above construction of θ_{ij} introduces the magnetic flux $-2\pi \times 2\theta N_a$ only to the plaquette with the origin O_θ shown in Fig. 2(c)³⁰. Since the string gauge ϕ_{ij} introduces the flux $\phi \times (1 - N_x N_y)$ to the plaquette with the origin O_ϕ while ϕ to the others as described above, one gets a condition of the uniformity of the magnetic field as $e^{i2\pi\phi(1 - N_x N_y) - i2\theta N_a} = e^{i2\pi\phi}$. Since $N_\phi = \phi N_x N_y$, this condition is consistent with the relation $1/\nu + \theta/\pi = \text{const}$.

IV. ENERGY GAP

By the above setup, we numerically diagonalize the Hamiltonians. In the following, we set $N_x = N_y = 10$, $t = -1$, $V = 5$ and $\vec{\eta} = \vec{0}$ unless otherwise stated. We assume that the states are degenerate if the energy difference is less than 0.001.

In Figs. 3(a)-(c), we plot the energies of a series that includes the $\nu = p$ IQH state ($p = 1, 2, 3$) as a function of $1/\nu$. We show the data for $\theta = (n/m)\pi$ with various m and n ($m \leq 7$). The data points with different colors are eigenvalues of H with the different dimensions. Figures 3(a)-(c) show that the gap behaves smoothly for a dense set of Hamiltonians. The energies of the ground state are also smooth, see the inset in Fig. 3(a).

Let us first consider a series of the $\nu = 1$ IQH state, which includes the Laughlin state. We here consider only $0 \leq \nu$ since a system of $\nu < 0$ is trivially mapped to that

of $0 < \nu$. In Fig. 3(a), the 3-fold degenerated ground state is obtained at $\nu = 1/3$, which is consistent with the lattice analogue of the Laughlin state³⁸. This state is adiabatically connected to the $\nu = 1$ IQH state. Note that, however, the ground state degeneracy N_D changes wildly, see Fig. 3(d). At $1/\nu = 0$, the gap closing occurs, which suggests the Nambu-Goldstone modes associated with the superconductivity of hard-core bosons³⁹. In Fig 3(a), the results without the electron-electron interactions are also shown. While the ground states of anyons or bosons are gapped because of their hard-core nature, the gap at $\nu = 1/3$ vanishes since the system reduces to the partially filled lowest Landau band of free fermions. It implies that the interaction is crucially important only for the FQH states of fermions. In Fig. 4, the energy spectra as functions of the interaction V are shown. The FQH states remain gapped with the same topological degeneracy for a wide range of V apart from the point $V = 0$ in Fig. 4(c). Inclusion of the finite interaction V induces the gap at this point, which is consistent with the gapped Laughlin state. Although the discussion of the thermodynamic limit is an open question, our adiabatic heuristic argument for the fixed system size includes important scientific information.

As for the other series in Figs. 3(b) and (c), one can also see that the gaps remain open for each region $0 < 1/\nu$ and $1/\nu < 0$ although their topological degeneracy changes irregularly [see Figs. 3(e) and (f)]. The excitation gap closes at $1/\nu = 0$ in both figures, which is consistent with the emergence of the anyon superconductivity³³⁻³⁵ of $\theta = (3/2)\pi$ and $\theta = (4/3)\pi$, respectively.

The numerical results in Figs. 3 suggest that the adi-

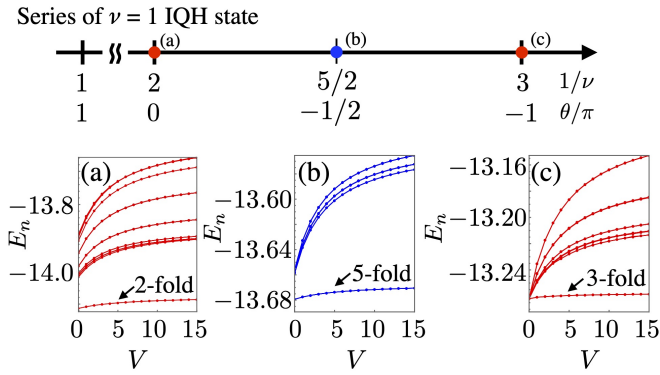


FIG. 4. Energy spectra are shown as functions of the interaction V for (a) the Boson FQH state at $\nu = 1/2$, (b) the anyon FQH state at $\nu = 2/5$ and (c) the Fermion FQH state at $\nu = 1/3$. They are included in a series of the $\nu = 1$ IQH state. We set $t = -1$ and $N_x \times N_y = 10 \times 10$. The lowest forty states are shown in each figure.

adiabatic heuristic principle remains valid for a series that includes $\nu = p$ IQH state for general integer p . It also suggests the realization of the anyon superconductivity of $\theta = (1 + 1/p)\pi$ by trading all the external magnetic flux for the statistical one.

Since $1/\nu \propto \phi$, where $\phi = N_\phi/(N_x N_y)$ is the number of the flux per plaquette, this unusual but adiabatic behavior, in a sense that the gap remains open, is similar to the Azbel-Hofstadter problem^{40–42} for the weak magnetic field limit. It implies that the adiabatic invariant of the evolution can be given by the Chern number of the ground state multiplet. This is correct as we discuss below.

V. ADIABATIC INVARIANT

As for the gapped ground state multiplet of anyons, we calculate the many-body Chern number⁵

$$C = \frac{1}{2\pi i} \int_{T^2} d^2\eta F, \quad (5)$$

where $T^2 = [0, 2\pi] \times [0, 2\pi]$, $F = (\partial A_y / \partial \eta_x) - (\partial A_x / \partial \eta_y)$, $A_{x(y)} = \text{Tr}[\Phi^\dagger (\partial \Phi / \partial \eta_{x(y)})]$ and $\Phi = (|G_1\rangle \cdots, |G_{N_D}\rangle)$ is a ground state multiplet. In the numerical calculation, we use the method proposed in Ref. 43.

In Figs 5(a-c), we plot C for the systems of the same setting as Figs. 3(a-c). Although the dimensions of the multiplet changes wildly, the Chern number C remains the same. It suggests that C is an adiabatic invariant of the evolution. As for a series that includes the $\nu = p$ IQH state, we numerically obtain

$$C = \text{sgn}(\nu) \times p, \quad (6)$$

where $\text{sgn}(x)$ is the sign function. For $\nu > 0$, Eq. (6) is natural since the $\nu = p$ IQH state is included. However,

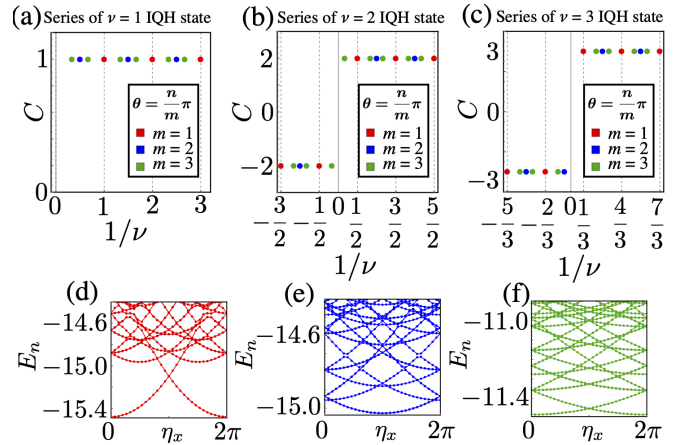


FIG. 5. (a)-(c) Chern number C of the degenerated ground state multiplet are shown as functions of $1/\nu$. In (a), (b) and (c), we consider the systems in the same setting as Fig. 3(a), (b) and (c), respectively. (d)-(f) Spectral flows at $1/\nu = 0$ for each series. We set $\eta_y = 0$. The statistics parameter is given by (d) $\theta/\pi = 2$, (e) $\theta/\pi = 3/2$ and (f) $\theta/\pi = 4/3$, respectively.

the case of $\nu < 0$ is non-trivial since it does not include any simple state.

While the energy of the QH systems is almost independent of $\vec{\eta}$, the spectral flows at $1/\nu = 0$ exhibit the strong $\vec{\eta}$ dependences, see Figs. 5(d-f). They indicate the absence of the energy gap at $1/\nu = 0$, which implies the Nambu-Goldstone modes of the anyon superconductors.

VI. TOPOLOGICAL DEGENERACY

As mentioned above, the ground state degeneracy changes wildly during the evolution as shown in Figs. 3(d-f). The fermion FQH state at $\nu = p/q$ is q -fold degenerated⁴⁴ but this pattern does not hold in the anyonic systems; the QH state with $(\nu, \theta/\pi) = (1, 1/2)$ in Fig. 3(e), for example, has 4-fold degeneracy. We address this issue analytically below.

Let us consider a continuous translational invariant system of the size $L_x \times L_y$ with external magnetic field $B = \phi_0 N_\phi / (L_x L_y)$. The results obtained below is valid even for lattice models as long as ϕ is sufficiently small, i.e., the magnetic length becomes much larger than the lattice constant. The statistics of anyons is set $\theta = (n/m)\pi$ and a translation operator of center-of-mass is given by $T(\mathbf{a}) = \exp\{(i/\hbar) \sum_i \mathbf{K}_i \cdot \mathbf{a}\}$, where $\mathbf{K}_i = \mathbf{p}_i + e\mathbf{A}(\mathbf{r}_i) - eB\mathbf{e}_z \times \mathbf{r}_i$ ^{44–46}. Since the interactions of the system including the statistical vector potential²¹ are given by the relative coordinates of anyons, $T(\mathbf{a})$ commutes with the Hamiltonian H . Noting that $T(\mathbf{b})^{-1}T(\mathbf{a})^{-1}T(\mathbf{b})T(\mathbf{a}) = e^{i\frac{e}{\hbar}B(\mathbf{a} \times \mathbf{b})N_a}$, let us now assume the followings

$$\rho_i^{-1}T(\mathbf{a})^{-1}\rho_i T(\mathbf{a}) = e^{i\frac{e}{\hbar}B(\mathbf{a} \times L_y \mathbf{e}_y)} \quad (7)$$

$$T(\mathbf{b})^{-1}\tau_i^{-1}T(\mathbf{b})\tau_i = e^{i\frac{e}{\hbar}B(L_x\mathbf{e}_x \times \mathbf{b})}, \quad (8)$$

since each loop given by Eqs. (7) and (8) does not enclose the other anyons.

Equation (1) implies $[\tau_i^m, \rho_j] = 0$. (The proof for any i and j is given in Appendix A). Then by defining $\mathcal{T}_A \equiv T(\frac{1}{m}\frac{L_y}{N_\phi}\mathbf{e}_y)$, which satisfies

$$[\mathcal{T}_A, \tau_i^m] = [\mathcal{T}_A, \rho_i] = 0, \quad (9)$$

let us take the simultaneous eigenstate $|\psi_0\rangle$, which satisfies $H(\vec{\eta})|\psi_0\rangle = E(\vec{\eta})|\psi_0\rangle$ and $\mathcal{T}_A|\psi_0\rangle = e^{i\lambda}|\psi_0\rangle$ with λ real. Here, the twisted boundary angles $\vec{\eta}$ are specified by τ_i^m and ρ_i with Eqs. (3) and (4). Further defining $\mathcal{T}_B \equiv T(\frac{L_x}{N_\phi}\mathbf{e}_x)$ and $\mathcal{T}_C \equiv \tau_1 T(\frac{n}{m}\frac{L_x}{N_\phi}\mathbf{e}_x)$, we define a new state $|\psi_{s,t}\rangle \equiv \mathcal{T}_B^s \mathcal{T}_C^t |\psi_0\rangle$. While \mathcal{T}_B and \mathcal{T}_C commute with τ_i^m and ρ_i , we have

$$\mathcal{T}_A \mathcal{T}_B = \mathcal{T}_B \mathcal{T}_A e^{i2\pi\frac{1}{m}\nu}, \quad (10)$$

$$\mathcal{T}_A \mathcal{T}_C = \mathcal{T}_C \mathcal{T}_A e^{i2\pi(\frac{1}{m} + \nu\frac{n}{m^2})}. \quad (11)$$

It implies $H(\vec{\eta})|\psi_{s,t}\rangle = E(\vec{\eta})|\psi_{s,t}\rangle$ and $\mathcal{T}_A|\psi_{s,t}\rangle = e^{i\lambda}e^{i2\pi f_{s,t}}|\psi_{s,t}\rangle$ with

$$f_{s,t} = \frac{\nu s + (1 + \nu\theta/\pi)t}{m} = \frac{\nu}{pm}(p(s+t) + t), \quad (12)$$

where $\nu = p/[p(1-\theta/\pi)+1]$ is used at the last part. Thus, the topological degeneracy N_{TD} is given by the number of pairs (s, t) that give different values of $f_{s,t} \bmod 1$. Since pm/ν is always integer, one obtains $N_{\text{TD}} = pm/|\nu|$. Using Eq. (6) and $M = m$ (irreducible representation), we have

$$N_{\text{TD}} = MC/\nu. \quad (13)$$

This is consistent with the obtained ground state degeneracy shown in Fig. 3(d-f). Anyon nature shown in Eq. (11) gives the extra degeneracy compared with the fermionic standard case⁴⁴.

VII. GENERALIZED STREDA FORMULA

Taking difference of Eq. (13) for two possible cases in a series, one obtains $\Delta N_{\text{TD}}/\Delta(M/\nu) = C$, where we assume the Chern number C is the invariant. Since $M/\nu = MN_x N_y \phi / N_a$ with ϕ the number of the flux per plaquette, we finally have

$$\frac{\Delta(N_p/N'_{\text{site}})}{\Delta\phi} = C, \quad (14)$$

where $N_p \equiv N_{\text{TD}}N_a$ is the ‘‘parton’’ number corrected by the topological degeneracy and $N'_{\text{site}} \equiv MN_x N_y$ is the extended number of sites due to the non-Abelian nature of the representation. This is a *generalized* Streda formula for anyons. Note that Eq. (14) for fermions ($M = 1$, $\nu = p/q$, $N_{\text{TD}} = q$, $C = p$) reduces to the standard Streda formula⁴⁷. When one includes a reducible representation of the braid group, i.e., $M = tm$ with $2 \leq t$ (t : integer), the degeneracy N_{TD} increases by t times. Therefore, Eqs. (13) and (14) holds generally.

VIII. CONCLUSION

In this Letter, the adiabatic heuristic principle for the QH states is demonstrated on a torus numerically. The emergence of the anyon superconducting states is also suggested. The Chern number of the ground state multiplet serves as the adiabatic invariant of the evolution although their degeneracy changes wildly. The anyon nature brings the extra multiplicity to the topological degeneracy. It results in a generalized Streda formula that follows from the translational invariance. Extensions of this adiabatic principle on a torus can be useful to characterize the non-Abelian FQH states.

ACKNOWLEDGMENTS

We thank the Supercomputer Center, the Institute for Solid State Physics, the University of Tokyo for the use of the facilities. The work is supported in part by JSPS KAKENHI Grant Numbers JP17H06138 (K.K., Y.H.), and JP19J12317 (K.K.).

Appendix A: Constraints on statistical phase

In this appendix, we derive the relation $1/\nu + \theta/\pi = \text{const.}$ from the braid group analysis on a torus. Also, a proof of $[\tau_i^m, \rho_j] = 0$ for any i and j is also given here.

In the main text, we denote the generators of the braid group on a torus by σ_i , τ_i and ρ_i . They satisfy the following relations^{13,31,32}:

$$\tau_{i+1}^{-1}\rho_i\tau_{i+1}\rho_i^{-1} = (\sigma_i^{-1})^2, \quad (A1)$$

$$\rho_1^{-1}\tau_1^{-1}\rho_1\tau_1 = \sigma_1 \cdots \sigma_{N_a-1}\sigma_{N_a-1} \cdots \sigma_1 e^{i\frac{e}{\hbar}BL_xL_y}, \quad (A2)$$

$$\tau_{i+1} = \sigma_i^{-1}\tau_i\sigma_i^{-1}e^{i\frac{e}{\hbar}(\alpha_{i+1}-\alpha_i)}, \quad (A3)$$

$$\rho_{i+1} = \sigma_i\rho_i\sigma_i e^{i\frac{e}{\hbar}(\beta_{i+1}-\beta_i)}, \quad (A4)$$

where α_i and β_i are real numbers. Equation (A1) is the same as Eq. (1). The derivations of Eqs. (A3) and (A4) are given in Appendix B.

Substituting $\sigma_i = e^{i\theta}\mathbf{1}_M$ into Eqs. (A1), (A2), (A3) and (A4), we have

$$\rho_i\tau_{i+1} = \tau_{i+1}\rho_i e^{-i2\theta}, \quad (A5)$$

$$\rho_1\tau_1 = \tau_1\rho_1 e^{i2(N_a-1)\theta+i2\pi N_\phi}, \quad (A6)$$

$$\tau_{i+1} = \tau_i e^{-i2\theta} e^{i\frac{e}{\hbar}(\alpha_{i+1}-\alpha_i)}, \quad (A7)$$

$$\rho_{i+1} = \rho_i e^{i2\theta} e^{i\frac{e}{\hbar}(\beta_{i+1}-\beta_i)}. \quad (A8)$$

Here, we note that the representations

$$\tau_j = e^{i\frac{e}{\hbar}\alpha_j} e^{-i2\theta(j-1)} W_x, \quad (A9)$$

$$\rho_j = e^{i\frac{e}{\hbar}\beta_j} e^{i2\theta(j-1)} W_y, \quad (A10)$$

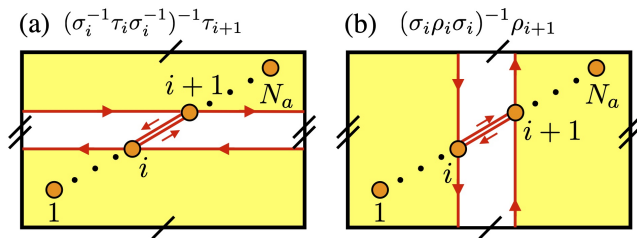


FIG. 6. Closed paths defined by (a) $(\sigma_i^{-1}\tau_i\sigma_i^{-1})^{-1}\tau_{i+1}$ and $(\sigma_i\rho_i\sigma_i)^{-1}\rho_{i+1}$.

satisfy the relations in Eqs. (A5), (A6), (A7) and (A8). Substituting Eq. (A7) into Eq. (A5), one gets

$$\rho_i\tau_j = \tau_j\rho_i e^{-i2\theta}. \quad (\text{A11})$$

If $\theta/\pi = n/m$, it reduces to $[\tau_i^m, \rho_j] = 0$. Comparing Eq. (A11) for $i = j = 1$ with Eq. (A6), we get

$$e^{i2\theta N_a + i2\pi N_\phi} = 1. \quad (\text{A12})$$

It implies that $\theta/\pi + 1/\nu = 2\pi s/N_a$ with s integer.

Appendix B: Noncontractible loops on a torus

In this appendix, we prove Eqs. (A3) and (A4). If the magnetic flux is absent, the relations of the braid group are given as^{13,28}

$$\tau_{i+1} = \sigma_i^{-1}\tau_i\sigma_i^{-1}, \quad (\text{B1})$$

$$\rho_{i+1} = \sigma_i\rho_i\sigma_i. \quad (\text{B2})$$

Note that $(\sigma_i^{-1}\tau_i\sigma_i^{-1})^{-1}\tau_{i+1}$ and $(\sigma_i\rho_i\sigma_i)^{-1}\rho_{i+1}$ move anyons along closed loops shown in Figs. 6(a) and (b), respectively. Therefore, if the magnetic field described by the vector potential $\mathbf{A}(\mathbf{r})$ is present, $(\alpha_{i+1} - \alpha_i)/\phi_0$ and $(\beta_{i+1} - \beta_i)/\phi_0$ fluxes penetrate each closed paths, respectively, where $\alpha_i = \oint_{L_{\tau_i}} d\mathbf{r} \cdot \mathbf{A}(\mathbf{r})$, $\beta_i = \oint_{L_{\rho_i}} d\mathbf{r} \cdot \mathbf{A}(\mathbf{r})$, and $L_{\tau_i(\rho_i)}$ is the path given by $\tau_i(\rho_i)$. Then we obtain Eqs. (A3) and (A4).

-
- ¹ K. v. Klitzing, G. Dorda, and M. Pepper, Phys. Rev. Lett. **45**, 494 (1980).
² D. C. Tsui, H. L. Stormer, and A. C. Gossard, Phys. Rev. Lett. **48**, 1559 (1982).
³ D. J. Thouless, M. Kohmoto, M. P. Nightingale, and M. den Nijs, Phys. Rev. Lett. **49**, 405 (1982).
⁴ M. Kohmoto, Annals of Physics **160**, 343 (1985).
⁵ Q. Niu, D. J. Thouless, and Y.-S. Wu, Phys. Rev. B **31**, 3372 (1985).
⁶ M. V. Berry, Proceedings of the Royal Society of London. A. Mathematical and Physical Sciences **392**, 45 (1984).
⁷ R. B. Laughlin, Phys. Rev. Lett. **50**, 1395 (1983).
⁸ X. G. Wen, Phys. Rev. B **40**, 7387 (1989).
⁹ D. Arovas, J. R. Schrieffer, and F. Wilczek, Phys. Rev. Lett. **53**, 722 (1984).
¹⁰ F. D. M. Haldane, Phys. Rev. Lett. **51**, 605 (1983).
¹¹ B. I. Halperin, Phys. Rev. Lett. **52**, 1583 (1984).
¹² X.-G. Wen, Advances in Physics **44**, 405 (1995).
¹³ T. Einarsson, Phys. Rev. Lett. **64**, 1995 (1990).
¹⁴ M. Oshikawa and T. Senthil, Phys. Rev. Lett. **96**, 060601 (2006).
¹⁵ M. Sato, M. Kohmoto, and Y.-S. Wu, Phys. Rev. Lett. **97**, 010601 (2006).
¹⁶ R. Willett, J. P. Eisenstein, H. L. Stormer, D. C. Tsui, A. C. Gossard, and J. H. English, Phys. Rev. Lett. **59**, 1776 (1987).
¹⁷ G. Moore and N. Read, Nuclear Physics B **360**, 362 (1991).
¹⁸ N. Read and E. Rezayi, Phys. Rev. B **59**, 8084 (1999).
¹⁹ A. Kitaev, Annals of Physics **303**, 2 (2003).
²⁰ C. Nayak, S. H. Simon, A. Stern, M. Freedman, and S. Das Sarma, Rev. Mod. Phys. **80**, 1083 (2008).
²¹ F. Wilczek, Phys. Rev. Lett. **49**, 957 (1982).
²² J. K. Jain, Phys. Rev. Lett. **63**, 199 (1989).
²³ J. K. Jain, Composite Fermions (Cambridge University Press, 2007).
²⁴ M. GREITER and F. WILCZEK, Modern Physics Letters B **04**, 1063 (1990).
²⁵ M. Greiter and F. Wilczek, Nuclear Physics B **370**, 577 (1992).
²⁶ Y.-S. Wu, Phys. Rev. Lett. **52**, 2103 (1984).
²⁷ Since the system of anyons is intrinsically a many-body problem, the construction of the pseudopotential projected into the lowest Landau level is impossible. Therefore, we choose a toroidal lattice model for the direct numerical demonstrations. This geometry is also suitable for evaluation of the topological numbers.
²⁸ J. S. Birman, Communications on Pure and Applied Mathematics **22**, 41 (1969).
²⁹ X. G. Wen, E. Dagotto, and E. Fradkin, Phys. Rev. B **42**, 6110 (1990).
³⁰ Y. Hatsugai, M. Kohmoto, and Y.-S. Wu, Phys. Rev. B **43**, 10761 (1991).
³¹ T. EINARSSON, Modern Physics Letters B **05**, 675 (1991).
³² D. LI, International Journal of Modern Physics B **07**, 2779 (1993).
³³ R. B. Laughlin, Phys. Rev. Lett. **60**, 2677 (1988).
³⁴ A. L. Fetter, C. B. Hanna, and R. B. Laughlin, Phys. Rev. B **39**, 9679 (1989).
³⁵ Y.-H. CHEN, F. WILCZEK, E. WITTEN, and B. I. HALPERIN, International Journal of Modern Physics B **03**, 1001 (1989).
³⁶ Y. Hatsugai, K. Ishibashi, and Y. Morita, Phys. Rev. Lett. **83**, 2246 (1999).
³⁷ The rule (i) ensures the local exchange operation. The rules (ii) and (iii) remove the artificial twisted boundary condition in the x - and y -direction caused by anyon fluxes, respectively. Necessity of the rule (iv) comes from order-

- ing vertical anyon strings of particles in the same x -axis position as the hopping anyon.
- ³⁸ K. Kudo, T. Kariyado, and Y. Hatsugai, *Journal of the Physical Society of Japan* **86**, 103701 (2017).
- ³⁹ S. C. ZHANG, *International Journal of Modern Physics B* **06**, 25 (1992).
- ⁴⁰ M. Y. Azbel, *ZhETF* 46, 929 (1964) [*J. Exp. Theor. Phys.* 19, 634 (1964)].
- ⁴¹ D. R. Hofstadter, *Phys. Rev. B* **14**, 2239 (1976).
- ⁴² Y. Hasegawa, Y. Hatsugai, M. Kohmoto, and G. Montambaux, *Phys. Rev. B* **41**, 9174 (1990).
- ⁴³ T. Fukui, Y. Hatsugai, and H. Suzuki, *Journal of the Physical Society of Japan* **74**, 1674 (2005).
- ⁴⁴ F. D. M. Haldane, *Phys. Rev. Lett.* **55**, 2095 (1985).
- ⁴⁵ J. Zak, *Phys. Rev.* **134**, A1602 (1964).
- ⁴⁶ R. Tao and F. D. M. Haldane, *Phys. Rev. B* **33**, 3844 (1986).
- ⁴⁷ P. Streda, *Journal of Physics C: Solid State Physics* **15**, L717 (1982).